

# Biomimetic Radar Target Recognition Based on Hypersausage Chains

Huan-Huan Zhang and Pei-Yu Chen

The School of Electronic Engineering  
Xidian University, Xi'an, 710071, China  
hhzhang@xidian.edu.cn

**Abstract** — A biomimetic radar target recognition method is proposed in this paper. From a geometrical perspective, the high resolution range profiles of radar targets are considered as points in high-dimensional feature space. Hypersausage chains are used to cognize the low-dimensional manifold embedding in the high-dimensional space. The topological framework construction algorithm for a hypersausage chain is improved and described in detail. A procedure for a reasonable selection of the hypersphere radius is also involved, which guarantees both acceptable generalization capability and excellent rejection capability of the classifier. The performance of proposed method is compared with the commonly used support vector machine (SVM) method with a radial basis function kernel or a polynomial kernel. Simulation results show that our proposed method outperforms the SVM methods in anti-noise capability, generalization capability and especially rejection capability.

**Index Terms** — Biomimetic radar target recognition, high resolution range profiles, hypersausage chains, manifold.

## I. INTRODUCTION

With the widespread application of high resolution radars, high resolution range profile (HRRP) of radar targets becomes more and more accessible. HRRP carries information of target scattering centers distribution along the radar pointing direction, which reflects details of target structure such as scatterer centers strength, scatterer centers position, target size and so on. Therefore, HRRP plays an increasingly important role in the field of radar automatic target recognition (RATR) [1]–[5].

There is a common process flow in a typical radar HRRP target recognition system. Provided that the wide band electromagnetic scattering field and the raw HRRP of the target is obtained, a preprocessing procedure, which contains alignment, localization, averaging and normalization, will be carried out firstly to improve the quality of raw HRRP. Then a feature extraction procedure is used to select proper feature vectors for the classifier. Four kinds of feature vectors are frequently

used in existing literature: 1) HRRP after preprocessing procedure, this means classification procedure is conducted directly after preprocessing. 2) Transformation of HRRP, such as differential power spectrum [6], bispectrum [7], [8], higher order spectra [9] and so on. All of these features can eliminate the sensitivity of the HRRP to the translation of target in the range window. 3) Target structure information extracted from HRRP, such as the amplitude of scatterer centers, scatterer centers position, target length and so on. 4) Dimensionality reduction of HRRP using principal component analysis (PCA), linear discriminant analysis (LDA), neighborhood preserving projections (NPP) [10] and so on. These dimensionality reduction methods can also be used after 2) or 3). The application of these methods can avoid the curse of dimensionality and facilitate the classifiers. It can be conclude that the sensitivity of HRRP to translation can be eliminated or the dimensionality of HRRP vectors can be reduced based on the feature vectors in 2) to 4). But some transformation methods and dimensionality reduction methods will cause loss of information and influence the recognition accuracy. So provided that the preprocessing procedure is done well enough to eliminate the sensitivity of HRRP to translation and the classifier is efficient to handle high dimensional data (It can be seen that the proposed method is very convenient to deal with high dimensional data), we directly use the HRRP after preprocessing procedure as feature vectors in this paper. Finally the classifier will give the recognition result by using the feature vectors.

Many traditional statistical learning methods have been used as classifier in radar target recognition, such as neural networks (NN) [11]–[13], genetic programming [14], support vector machine (SVM) [15]–[18] and so on. These methods always aim at best distinguishing the samples of different classes based on their differences in feature space. Taking the SVM method as an example, it maps the training samples to a higher dimensional space and finds a linear separating hyperplane with the maximal margin for them. However, people cognize things in a very different manner. When you see a new thing, your first response is that you are not familiar with

it rather than to compare it with things you know. The latter is the manner in which traditional statistical learning methods do. This reflects that people focus on cognizing things whereas traditional statistical learning methods are concerned with distinction of things. It is not difficult to foresee that the latter will suffer from two drawbacks in radar target recognition. First, if encountering a new target without learning, it cannot realize that the target is not trained. It can only assign it to one of the trained target constrainedly, which makes the rejection capability of traditional statistical learning methods very poor. Second, if a new target needs to be learned, we must add its samples to the database and retrain samples of all classes. This makes the efficiency of traditional statistical learning methods very low when training new samples. Imitating the cognitive nature of human, a biomimetic pattern recognition method based on hypersausage chain was proposed [19]–[21]. In this paper, we improve this method and apply it to radar target recognition. The experiment results show that the proposed method has better anti-noise capability, generalization capability and especially rejection capability compared with the SVM method. It is worth mentioning that the proposed method works in optical scattering region. For the radar target recognition method in resonance region, there also exist some works which focus on discriminating unknown targets from known targets [22], [23].

The remainder of this paper is organized as follows. Section II describes the raw HRRP database prepared for radar target recognition. In Section III, we introduce the biomimetic radar target recognition algorithm based on hypersausage chains. Section IV shows the experiments and results. Finally, section V gives some conclusions.

## II. DATA PREPARATION

A raw HRRP database is built for five scaled models (F15, F117, VFY218, plane model and missile model). Physical optical (PO) method [24]–[26] is employed to simulate the VV polarization backscattering field of them at an elevation angle of  $10^\circ$ . For the computation of F15, F117 and VFY218 models, the azimuth angle is changed continuously from  $0^\circ$  (nose-on direction) to  $90^\circ$  with an interval of  $0.4^\circ$ . For the simulation of the plane and missile models, 75 azimuth angles are selected randomly from  $0^\circ$  to  $90^\circ$ . In each angle, 201 frequencies from 8GHz to 12GHz with a frequency step of 20 MHz are calculated, yielding 4GHz bandwidth. Then the raw range profiles are obtained by inverse fast Fourier transform (FFT). At last, each raw range profile is normalized by their maximum and minimum so that values of each range profile are scaled to between 0 and 1.

It can be found through above description the database has 226 range profiles for F15, F117, VFY218 models separately and 75 range profiles for plane, missile models separately. In the experiment stage, we

will only use some range profiles of F15, F117, VFY218 models to train the classifier and the other range profiles will be used to test the performance of the classifier.

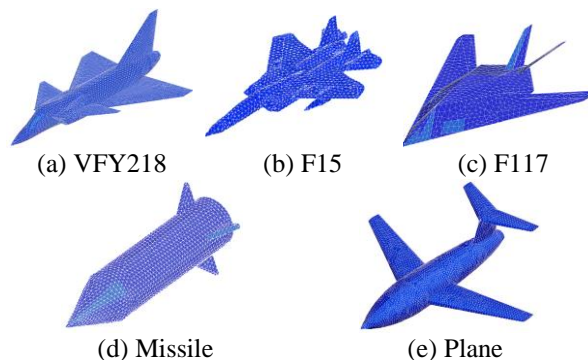


Fig. 1. Five meshed models.

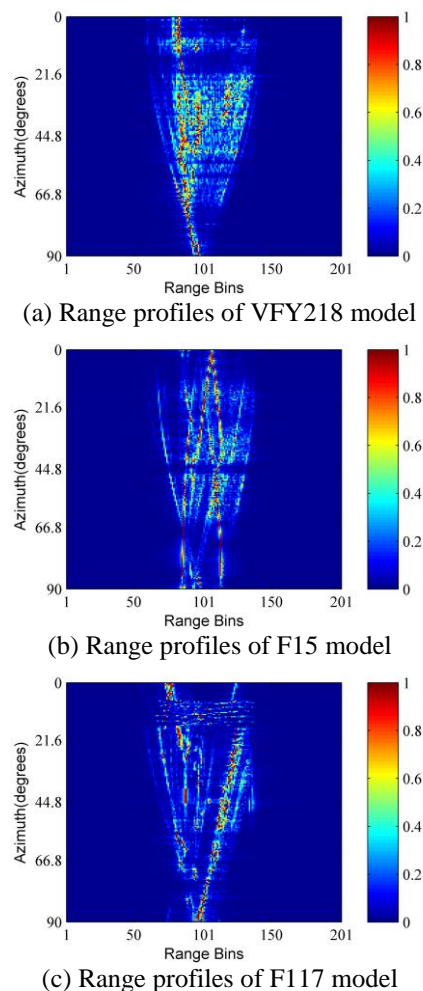


Fig. 2. Range profiles of three models.

The five scaled models are shown in Fig. 1. The sizes of them are shown in Table 1. By considering the

frequency range and the dimensions of the targets, we can find that they fall into optical scattering region. The normalized range profiles of F15, F117, VFY218 models are illustrated in Fig. 2. As evidenced by Fig. 2, the range profiles of targets are very sensitive to the azimuth angle, which implies that radar HRRP target recognition requires plenty of range profiles from various azimuth angles to guarantee reliable recognition accuracy. As mentioned in the introduction, the above normalized range profiles will be used directly as feature vectors for the classification experiment in Section IV.

Table 1: The dimensions of five targets

Targets	Length (m)	Width (m)	Height (m)	Scaling Ratio
VFY218	3.09	1.78	0.82	4.85
F15	3.00	2.10	0.66	6.48
F117	3.00	2.03	0.37	6.69
Missile	2.99	1.17	1.17	1.00
Plane	3.00	2.97	0.87	9.53

### III. BIOMIMETIC RADAR TARGET RECOGNITION BASED ON HYPERSAUSAGE CHAINS

#### A. Theory and principle

The theoretical basis of biomimetic pattern recognition is the principle of homology-continuity (PHC), which points out that samples from the same class change gradually and continuous variation sequences exist between any two samples of same class. This principle implies that biomimetic pattern recognition takes advantage of some prior knowledge of samples. It is obvious that the radar HRRP feature also obeys this principle. So the biomimetic pattern recognition method can be applied to radar target recognition problems. In the following of this paper, we will use biomimetic radar target recognition (BRTR) to call the proposed method.

For the realization of BRTR, a range profile from some class is considered to be a point in high-dimensional space. All the range profiles of the same class can be represented as a point set. Base on the PHC, neighboring points of the point set have strong correlations. This can produce observation which lies on low-dimensional manifold. So we can use some geometry to cover the low-dimensional manifold of a target if we want to cognize the target. In the context of radar target recognition, we believe that one-dimensional (1D) connectivity takes a major role among possible types of connectivity. So we consider a manifold resulted from a product of a hyper-sphere and a 1D continuous curve, where the 1D continuous curve represents the trend of the manifold and the hyper-sphere indicates the perturbation in other directions. For the sake of efficient implementation, a hypersausage chain (shortly HSN chain) formed by moving the center of a hypersphere

along a chain of line segments is used as an approximation model to this kind of manifold. It can be observed that such a hypersausage chain is composed of many sausage-like units, each of which stems from the product of a hypersphere with a line segment. This kind of sausage-like unit is termed as hyper sausage neuron (HSN). The 2D models of HSN chain and HSN are illustrated in Fig. 3, where  $\mathbf{x}_a$  and  $\mathbf{x}_b$  are the two nodes of the line segment,  $r$  is the radius of the hypersphere.

According to the above theory, the main task in the training stage of biomimetic radar target recognition is to find proper hypersausage chains to cover the low-dimensional manifold of different classes. This can be done in two steps. First, the chain of line segments, which is the topological framework of the HSN chain, must be constructed. Second, the radius of the hypersphere must be determined. III-B and III-C will introduce these two steps, respectively.

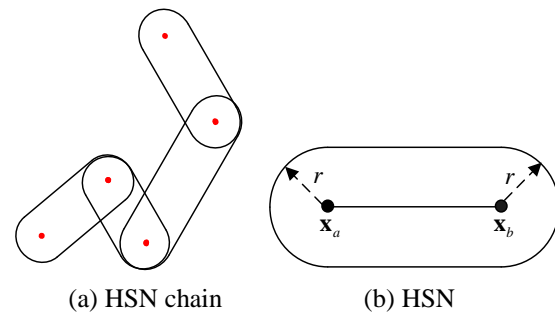


Fig. 3. 2D model of HSN chain and HSN.

#### B. Topological framework construction algorithm

First of all, we choose the HRRP vector of the first angle as the starting node of the first hyper sausage neuron. Then HRRPs of other angles can be sorted based on this reference point according to the sorting criterion that the mid HRRP vector is more close to the former HRRP vector than the latter one among three adjacent HRRP vectors. This guarantees that HRRP vectors in the high dimensional space change continuously. Using  $X$  to represent the set of ordered range profiles from some target, the aforementioned criterion can be described as:

$$X = \{ \mathbf{x}_i, \rho(\mathbf{x}_{i-1}, \mathbf{x}_i) \leq d < \rho(\mathbf{x}_{i-1}, \mathbf{x}_{i+1}) \} \quad (1)$$

$$i = 1, 2, \dots, Na,$$

where  $\mathbf{x}_i$  represents the  $i$ th range profiles.  $\rho(\mathbf{x}, \mathbf{y})$  refers to the Euclidean distance between vectors  $\mathbf{x}$  and  $\mathbf{y}$ .  $Na$  denotes the number of range profiles used as training data set. The topological framework of the HSN is formed by a subset of  $X$  whose elements are elaborately selected as the nodes of the hypersausage neurons and can reflect the trend of all the HRRP vectors in high-dimensional space. We use  $S$  to represent this subset, where  $S = \{ \mathbf{s}_i \}, i = 1, 2, \dots, n_1, n_1 < Na$ . Because the two

nodes of each hypersausage neuron is determined in the same manner and the start node of the latter neuron is the end node of the former neuron (the start node of the first neuron is the first HRRP vector in  $X$ , namely  $\mathbf{x}_1$ ), we will only take one hypersausage neuron as an example to introduce the method for its end node selection in the following of this section. The whole topological framework of the HSN will be constructed after the nodes of all hypersausage neurons are determined. The entire algorithm will be described at the end of this section.

Assuming that  $\mathbf{x}_j \in X$  refers to the start node of a neuron,  $\varepsilon_1$  represents the filter interval,  $\varepsilon_2$  denotes the disturbance tolerance,  $d$  is the Euclidean distance between current filtered HRRP vector and the start node,  $\mathbf{x}_{j+1}, \mathbf{x}_{j+2}, \dots, \mathbf{x}_{N_a}$  will be filtered sequentially to determine its end node. There are three typical cases in the process of filtering:

- 1) As illustrated in Fig. 4 (a), if the distance  $d$  increases continually and exceeds  $\varepsilon_1$ , the current filtered HRRP vector will be selected as the end node of the neuron.
- 2) Figure 4 (b) shows that the distance  $d$  decreases in the process of increasing and the decreased value is smaller than  $\varepsilon_2$ . This kind of decrease is a slight disturbance and does not influence the trends of topological framework of the HSN. So it can be tolerated and continue to filter the following HRRP vectors until  $d$  exceeds  $\varepsilon_1$ .
- 3) In Figs. 4 (c) and (d), the distance  $d$  increases to a value smaller than  $\varepsilon_1$  then decreases continually. If the decreasing value is greater than  $\varepsilon_2$ , the turning point will be considered as the end node of the neuron, and it is also the start node of next neuron. As in [19], the end node of the next neuron will be filtered from current HRRP vector for the purpose of accelerating computation. But this ignores the distribution of HRRP vectors between the turning point and current point. If the distribution of these points is very complicated, the topological framework obtained by original method may not describe the trends very well. Taking the case in Fig. 4 (d) as an example, the first point is the start node of current neuron and the second to tenth points will be filtered to find the end node of current neuron. From the second to fifth point, the distance  $d$  is increasing all the time but does not exceed  $\varepsilon_1$ . Then it decreases but the decreased value does not exceed  $\varepsilon_2$  from the sixth to ninth point until the tenth point. According to [19], the fifth point will be selected as the end node of current neuron. Then the filtering process will continue from the tenth point to find the end node of next neuron and the sixth to ninth points

are ignored. But it is obvious that the distance between the fifth and ninth point exceeds  $\varepsilon_1$  and the ninth point should be selected as the end node of the next neuron. So in order to acquire a more accurate topological framework, in this paper we choose the turning point as the end node of current neuron and the start point of the next neuron, meanwhile the end node of the next neuron will also be filtered from the turning point.

Based on the above analysis, the entire algorithm for the topological framework construction can be summarized in Table 2. It is necessary to point out that the selection of the filter interval  $\varepsilon_1$  and disturbance tolerance  $\varepsilon_2$  will affect the recognition effect of proposed method. If the nearest distance of all the samples is  $d_1$  and the farthest distance of them is  $d_2$ , we recommend choosing  $\varepsilon_1$  in the range of  $(d_1, d_2)$  by using cross-validation.  $\varepsilon_2$  is selected between a third and half of  $\varepsilon_1$ .

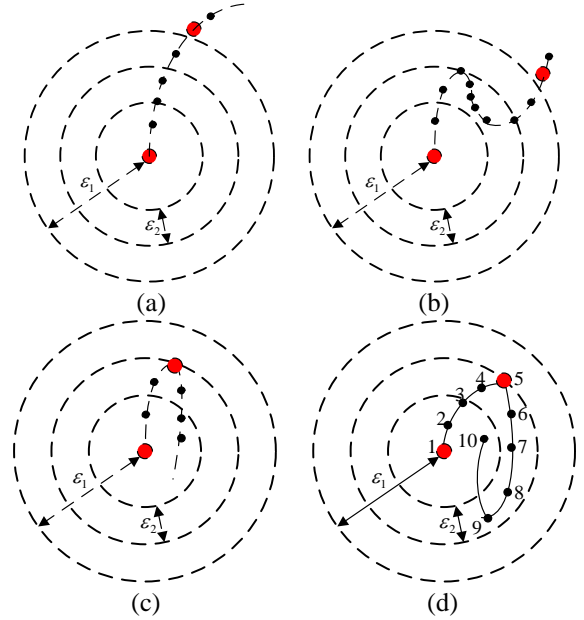


Fig. 4. Three typical cases in the construction of topological framework. The red points represent the nodes of current neuron. The black points denote the feature vectors not selected as nodes of current neuron.

### C. The radius of hypersphere

The topological framework describes the main trend of the HSN chain while the radius of the hypersphere decides its coverage area. A larger coverage area means better generalization capability of the classifier while a smaller one implies better rejection capability. So one can strengthen generalization or rejection capability by adjust the radius of the hypersphere. An instructive procedure for the selection of a proper radius will be given in the following of this section.

Table 2: The topological framework construction algorithm of HSN chain

**Input:** The set of ordered HRRP vectors corresponding to the HRRP of all angles:

$$X = \{\mathbf{x}_i, i = 1, 2, \dots, Na\}.$$

**Output:** The set of ordered HRRP vectors forming the topological framework of HSN:

$$S = \{\mathbf{s}_i | i = 1, 2, \dots, n_1, n_1 < Na\}.$$

*Initialization:*

1. Initialize the first feature vector  $\mathbf{x}_1$  as reference point  $\mathbf{s}_b$ , set  $\mathbf{s}_b = \mathbf{x}_1$ .
2. Save the first HRRP vector to the aforementioned set  $S$ , set  $S = \{\mathbf{x}_1\}$ .
3. Initialize  $\mathbf{s}_{\max} = \mathbf{0}$ , where  $\mathbf{s}_{\max}$  represents the farthest HRRP vector from the reference point.
4. Initialize  $d_{\max} = 0$ , where  $d_{\max}$  denotes the distance between  $\mathbf{s}_{\max}$  and the reference point.
5. Initialize  $i=2$ , where  $i$  refers to the number of next HRRP vector to be filtered in set  $X$ .

*Find the end node of a neuron and reinitialize:*

1. Filter the  $i$ th to  $N$ th HRRP vectors. The  $i$ th HRRP vector is recorded as  $\mathbf{s}$ , the Euclidean distance between  $\mathbf{s}$  and the reference point  $\mathbf{s}_b$  is  $d = \|\mathbf{s} - \mathbf{s}_b\|$ .
- 2.1 If  $d_{\max} < d < \varepsilon_1$ , set  $\mathbf{s}_{\max} = \mathbf{s}$ ,  $d_{\max} = d$ ,  $num=i$ ,  $i=i+1$ , go to step 1;
- 2.2 If  $d > d_{\max}$  and  $d > \varepsilon_1$ , save  $\mathbf{s}$  to set  $S$ , namely  $S = S \cup \{\mathbf{s}\}$ , reinitialize  $\mathbf{s}_b = \mathbf{s}$ ,  $\mathbf{s}_{\max} = \mathbf{0}$ ,  $d_{\max} = 0$ ,  $i=i+1$ , go to step 1;
- 2.3 If  $d \leq d_{\max}$  and  $d_{\max} - d < \varepsilon_2$ ,  $i=i+1$ , go to step 1;
- 2.4 If  $d \leq d_{\max}$  and  $d_{\max} - d > \varepsilon_2$ , save  $\mathbf{s}_{\max}$  to set  $S$ ,  $S = S \cup \{\mathbf{s}_{\max}\}$ , reinitialize  $\mathbf{s}_b = \mathbf{s}_{\max}$ ,  $d_{\max} = 0$ ,  $\mathbf{s}_{\max} = \mathbf{0}$ ,  $i=num$ , go to step 1.

First of all, the distance between a HRRP vector and a HSN is defined as follows:

$$d(\mathbf{x}, \overline{\mathbf{x}_a \mathbf{x}_b}) = \begin{cases} \|\mathbf{x} - \mathbf{x}_a\| & p(\mathbf{x}, \mathbf{x}_a, \mathbf{x}_b) < 0 \\ \|\mathbf{x} - \mathbf{x}_b\| & p(\mathbf{x}, \mathbf{x}_a, \mathbf{x}_b) > \|\mathbf{x}_b - \mathbf{x}_a\| \\ \sqrt{\|\mathbf{x} - \mathbf{x}_a\|^2 - p^2(\mathbf{x}, \mathbf{x}_a, \mathbf{x}_b)} & \text{otherwise} \end{cases} \quad (2)$$

As illustrated in Fig. 3 (b),  $\mathbf{x}_a$  and  $\mathbf{x}_b$  are the start node and end node of the HSN, respectively,  $p(\mathbf{x}, \mathbf{x}_a, \mathbf{x}_b)$  represents the projection of  $\mathbf{x}_a \mathbf{x}_b$  on the unit vector in the

direction of  $\overline{\mathbf{x}_a \mathbf{x}_b}$  and  $p(\mathbf{x}, \mathbf{x}_a, \mathbf{x}_b) = \left\langle \mathbf{x} - \mathbf{x}_a, \frac{\mathbf{x}_b - \mathbf{x}_a}{\|\mathbf{x}_b - \mathbf{x}_a\|} \right\rangle$ .

Then the distance between a HRRP vector and the HSN chain is defined as the nearest distance between the HRRP vector and all the neurons of the HSN chain. Finally, Radius can be computed by using different methods according to the number of training HRRP vectors:

- 1) A small number of training HRRP vectors

Find the farthest three samples from the topological framework of HSN chain. Average the distance between the framework and them and record it as  $r_1$ . The purpose of averaging operation is to relieve the influence of outlier. The radius is given as  $r_1 + \Delta r_1$ , where  $\Delta r_1$  is a small positive number.

- 2) A large number of training HRRP vectors

According to Section III-B,  $S$  refers to the subset whose elements construct the topological framework of HSN chain. We can use a set  $T=X-S$  to represent the remainder of  $X$ . The distances between every HRRP vector of  $T$  and the HSN chain can be computed and they constitute a set  $D_T = \{d_1, d_2, \dots, d_{n_2}\}$ .  $n_2$  is the number of HRRP vectors in set  $D_T$ . When  $n_2$  is large, the elements in  $D_T$  are considered to obey Gaussian distribution, namely:

$$P(d) = \frac{1}{\sqrt{2\pi}\sigma} e^{-d^2/2\sigma^2}. \quad (3)$$

The maximum likelihood estimation of  $\mu$  and  $\sigma$  are:

$$\hat{\mu} = \frac{1}{n_2} \sum_{j=1}^{n_2} d_j, \quad (4)$$

$$\hat{\sigma}^2 = \frac{1}{n_2} \sum_{j=1}^{n_2} (d_j - \hat{\mu})^2. \quad (5)$$

The radius  $r_2$  can be calculated by:

$$\int_0^{r_2} P(x) dx = 1 - \Delta r_2, \quad (6)$$

where  $\Delta r_2$  is a very small positive number.

#### D. Testing method

By constructing the topological framework and selecting proper radius, we can train a HSN chain for each target. Then the testing procedure is to judge whether a testing HRRP is in the coverage of some trained HSN chain. Firstly, we introduce a decision function  $f_{HSNC}(\mathbf{x})$  to indicate how close a testing HRRP  $\mathbf{x}$  is to a HSN chain:

$$f_{HSNC}(\mathbf{x}) = 2^{-d^2(\mathbf{x}, HSNC)/r^2} - 0.5. \quad (7)$$

Where  $d(\mathbf{x}, HSNC)$  denotes the distance between the testing HRRP and a HSN chain. If a testing HRRP  $\mathbf{x}$  is covered by a HSN chain of a target, the distance  $d(\mathbf{x}, HSNC)$  is smaller than  $r$ , this will result that

$f_{HSNC}(\mathbf{x}) > 0$ . Moreover, the smaller  $d(\mathbf{x}, HSNC)$  is, the closer  $f_{HSNC}(\mathbf{x})$  is to 0.5. On the contrary, if  $\mathbf{x}$  is outside the HSN chain,  $f_{HSNC}(\mathbf{x})$  will be less than zero. Now the testing method can be concluded as below:

Assuming that there are  $N$  kinds of targets, the HSN chain of them are noted as  $HSNC_1, HSNC_2, \dots, HSNC_N$ . The decision function  $f_{HSNC_i}(\mathbf{x})$  associated with a testing HRRP and the  $i$ th HSN chain is computed, where  $i = 1, 2, \dots, N$ . If all these decision functions are less than zero, this means that the testing HRRP belongs to none of the above HSN chain. Its corresponding target will be considered as unknown and rejected. If there is only one decision function greater than zero, the testing HRRP is exclusively covered by the corresponding HSN chain. The classifier will judge that the testing HRRP comes from the corresponding target. There is a troublesome case that the testing HRRP is covered by more than one HSN chain simultaneously. In this case, there will be more than one decision functions greater than zero. Based on the idea that the testing HRRP is generally more closed to the HSN chain of its corresponding target, the classifier will judge that the testing HRRP belongs to the target corresponding to the largest decision function value.

#### IV. EXPERIMENTS AND RESULTS

Several experiments are conducted to examine the performance of the proposed BRTR method. The results are compared with that of support vector machine method [27]. The SVM program is provided by LibSVM [28]. The training sets and testing sets of SVM are always the same as that of the proposed method. Both the polynomial kernel and the radial basis function (RBF) kernel are used as the kernel functions of SVM in each of the following experiments. The parameters of RBF kernel are selected according to the procedure recommended in [29] and reasonable results can always be obtained. Because the polynomial kernel has more parameters than the RBF kernel, it is difficult to select optimal parameters for it, which results that the RBF kernel usually has a better performance than polynomial kernel in our experiments. So we will only show the results of SVM with RBF kernel.

In the following experiment, we use  $P_c$  to represent correct recognition rate,  $P_r$  to denote correct rejection rate. The correct recognition rate is the probability of correctly classifying a known target. The correct rejection rate refers to the percentage of an unknown target rejected correctly. Here we use the terms “known” and “unknown” to indicate targets in the training database and those that are not.

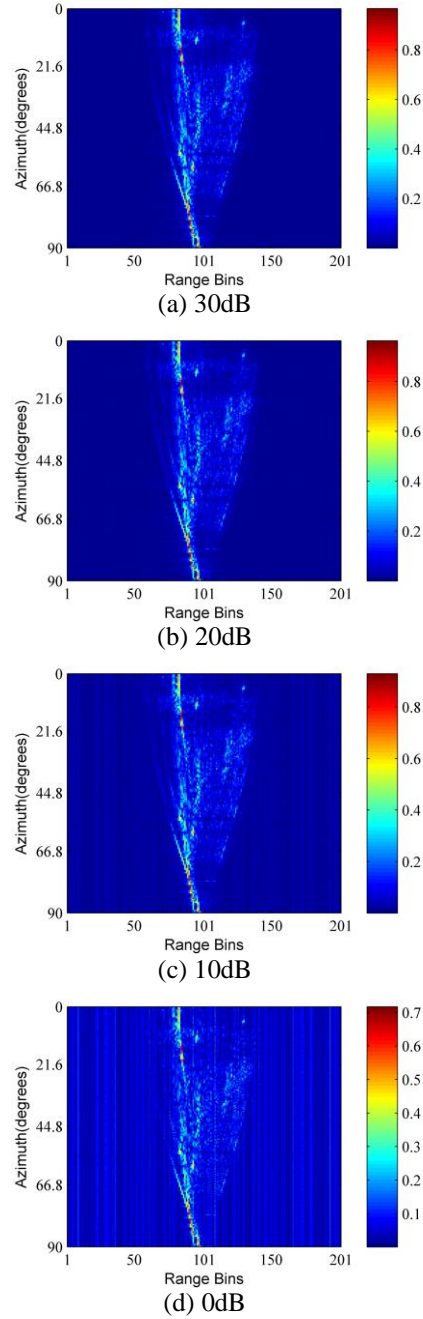


Fig. 5. Range profiles of VFY218 model with different noise level.

#### A. Anti-noise capability

The first experiment is designed to examine the anti-noise capability of the classifier. The scattered fields of VFY218, F15 and F117 models in frequency domain are contaminated by independent additive White Gaussian noise (AWGN) to achieve the signal to noise ratios (SNR) from 0 to 30dB with a 5dB increment. Then the

contaminated range profiles are obtained by inverse fast Fourier transform and normalized between 0 and 1. Figure 5 shows the contaminated range profiles of VFY218 at the noise levels of 0dB, 10dB, 20dB and 30dB. It is clear that the small values of range profiles are buried in noise when the SNR is low. In this experiment, the odd contaminated range profiles of each target are chosen as training set while the even ones are chosen as testing set, providing 113 different training vectors for each target and totally 339 different testing vectors at each SNR level.

The correct recognition rates against various SNR are demonstrated in Fig. 6. To obtain a correct recognition rate at some SNR, the training and testing processes are repeated 100 times with 100 independent AWGN realizations. Then the resultant 100 correct recognition rates are averaged as the final correct recognition rate  $P_c$ .

As it can be seen in Fig. 6, the correct recognition rate of BRTR method is very similar to that of SVM method when the SNR is above 15db. However, for the cases of SNR below 15db, the BRTR method slightly outperforms the SVM method. So we can conclude that the BRTR method is robust to noise and has a better performance than SVM method at a low SNR level.

## B. Generalization capability

Generally speaking, the more samples used in training stage, the better performance can be achieved in testing stage. However, it is impractical to build a huge training database for radar target recognition because of cost concerns. So a desired classifier should provide robust and acceptable accuracy when only limited training samples can be obtained.

In the second experiment, different amounts of range profiles from original data set of each model are used as training set to examine the generalization capability of the classifier. The training set of each target is selected from original data set of VFY218, F15 and F117 models with the interval varying from 2 to 6. And the increment is 1. The rest of range profiles from original data set are used as the test set. In other words, there are 113, 76, 57, 46, 38 range profiles for the training of each target and correspondingly 113×3, 150×3, 169×3, 180×3, 188×3 range profiles for testing. Here the decreasing of the training range profiles means increasing the azimuth interval of two neighboring training range profiles, which will reduce the correlations between training sets and testing sets.

The experiment results in Fig. 7 show that the correct recognition rates of BPTR and SVM method are above 96% when the number of training range profiles is more than half of the testing range profiles. But when the number of training range profiles decreases less than half of the testing range profiles, the correct recognition rate of SVM method decreases sharply while that of BPTR drops relatively slow. So the BPTR method is superior

to SVM method for small size of training set. In other words, the BPTR method has better generalization capability than SVM method.

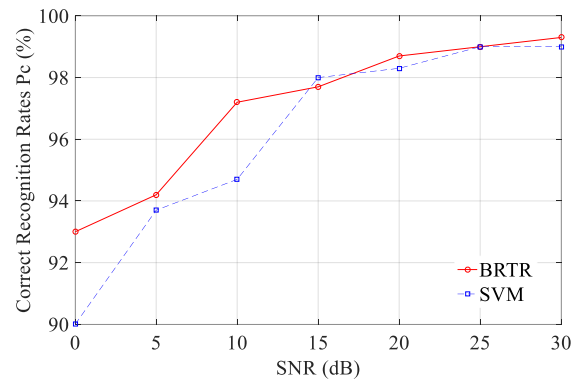


Fig. 6. Performance of biomimetic radar target recognition method and support vector machine method at different levels of SNR.

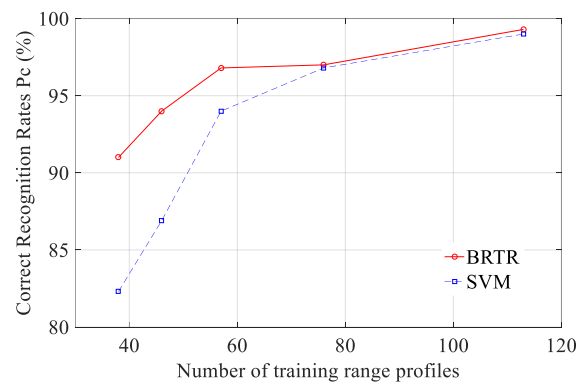


Fig. 7. Performance of biomimetic radar target recognition method and support vector machine method when the number of training and testing range profiles varies.

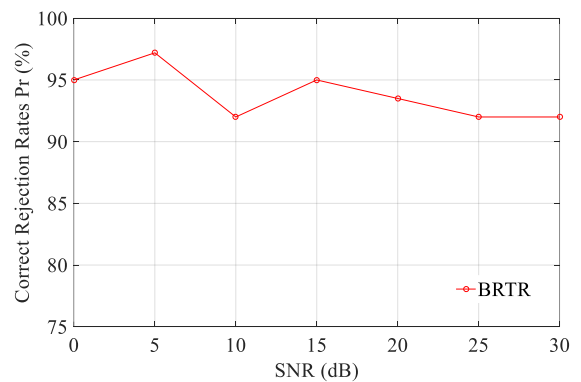


Fig. 8. Rejection capability of biomimetic radar target recognition method at different levels of SNR using the same training range profiles in the anti-noise capability experiment.

### C. Rejection capability

Most of the classifiers used for radar target recognition are trained and tested with known targets, but there exist targets which are not included in the training database in reality. Rejection of unknown targets is a very challenging problem not only in the field of radar HRRP recognition but also in the entire automatic target recognition community. Though rejection capability of radar automatic target recognition is of great importance, it does not attract enough attention. One of the most fascinating abilities of our proposed method is its rejection capability.

The third experiment is designed to examine this capability of the classifier. The training range profiles in the anti-noise experiment at different SNR levels are also chosen as the training set in this experiment. The 150 range profiles of two additional unknown targets (plane and missile model) constitute the testing set. It is necessary to point out that the parameters  $\varepsilon_1$  and  $\varepsilon_2$  are also the same as that in anti-noise experiment, which guarantees that the proposed method can have good rejection capability without sacrificing the anti-noise capability. The experiment results in Fig. 8 show that our proposed method can achieve over ninety percent correct rejection rate, which overcomes the weakness of the traditional statistical learning methods. Moreover, it can be observed that the rejection performance becomes slightly better with lower SNR levels. The reason is that when the SNR is high, a HRRP of the two unknown targets at some azimuth angle may be similar to some HRRP of the known targets since the size of all the targets are similar and they share some common features. However, when the SNR is very low, the HRRPs will be contaminated by noise severely. The similarity of HRRPs between the known targets and unknown targets will also be weakened.

All the above experiments are carried out on a PC with 2.83 GHz CPU and 8 GHz RAM. The parameters  $\varepsilon_1=0.6$  and  $\varepsilon_2=0.25$  for VFY218, F15 and F117 models. A large number of training HRRP vectors is assumed and  $\Delta r_2=0.001$ , resulting in that  $r_2$  equals to 0.66, 0.64 and 0.54 for VFY218, F15 and F117 models, respectively. The average training time of the proposed method and the SVM method are 658 ms and 260 ms respectively for different SNR levels. The average testing time of them are 46 ms and 42 ms, respectively.

### V. CONCLUSION

A biomimetic radar target recognition method based on hypersausage chains has been proposed and its performance was investigated. Distinct from the distinguishing scheme of traditional statistical learning methods, the proposed method aims at cognizing targets, which is inspired by the cognition nature of human. From a geometrical point of view, the HRRP vectors are

considered to be points in high dimensional space. A hypersausage chain is utilized to optimally cover the points of each target. Three experiments have been conducted and the results show that the proposed method is more robust to noise and the size of training sets compared with the SVM method. Moreover, it is worth mentioning that the proposed method has an excellent rejection capability which is a basic capability of human. This capability is extremely important for a real radar target recognition system. An additional advantage of the proposed method is that it does not need to retrain all the samples in the database when the samples of a new target are added to the database, while the traditional statistical learning methods must retrain all the samples when any new target is included into the database.

### ACKNOWLEDGMENT

The authors would like to thank the support of National Natural Science Foundation of China under Grant 61701376, China Postdoctoral Science Foundation under Grant 2017M613071, 2018T111016, Open Project Foundation of the State Key Laboratory of Millimeter Waves under Grant K201808, Open Project Foundation of Key Laboratory of High-Speed Circuit Design and EMC, Ministry of Education. The authors would also like to thank the earnest work of the editors and anonymous reviewers.

### REFERENCES

- [1] H. J. Li, Y. D. Wang, and L. H. Wang, "Matching score properties between range profiles of high-resolution radar targets," *IEEE Trans. Antennas Propag.*, vol. 44, no. 4, pp. 444-452, Apr. 1996.
- [2] R. A. Mitchell and J. J. Westerkamp, "Robust statistical feature based aircraft identification," *IEEE Trans. Aerosp. Electron. Syst.*, vol. 35, no. 3, pp. 1077-1094, July 1999.
- [3] Z. H. Guo and S. H. Li, "One-dimensional frequency-domain features for aircraft recognition from radar range profiles," *IEEE Trans. Aerosp. Electron. Syst.*, vol. 46, no. 4, pp. 1880-1892, Oct. 2010.
- [4] H. H. Zhang, D. Z. Ding, Z. H. Fan, and R. S. Chen, "Adaptive neighborhood preserving discriminant projection method for HRRP based radar target recognition," *IEEE Antennas Wirel. Propag. Lett.*, vol. 14, pp. 650-653, 2015.
- [5] L. Du, H. He, L. Zhao, and P. Wang, "Noise robust radar HRRP target recognition based on scatterer matching algorithm," *IEEE Sensors Journal*, vol. 16, no. 6, pp. 1743-1753, Mar. 2016.
- [6] Z. H. Guo and S. H. Li, "Radar target recognition using the differential power spectrum," in *Conf. Rec. 2005 IEEE Int. Conf. Communications and Signal Processing*, pp. 385-387, 2005.
- [7] I. Jouny, E. D. Garber, and R. L. Moses, "Radar

- target identification using the bispectrum: A comparative study," *IEEE Trans. Aerosp. Electron. Syst.*, vol. 31, no. 1, pp. 69-77, Jan. 1995.
- [8] B. Pei, Z. Bao, and M. D. Xing, "Logarithm bispectrum-based approach to radar range profile for automatic target recognition," *Pattern Recognition*, vol. 35, no. 11, pp. 2643-2651, Nov. 2002.
- [9] L. Du, H. W. Liu, Z. Bao, and M. D. Xing, "Radar HRRP target recognition based on higher order spectra," *IEEE Trans. Signal Process.*, vol. 53, no. 7, pp. 2359-2368, July 2005.
- [10] X. Yu, X. Wang, and B. Liu, "Supervised kernel neighborhood preserving projections for radar target recognition," *Signal Processing*, vol. 88, no. 9, pp. 2335-2339, Sept. 2008.
- [11] I. Jouny, F. D. Garber, and S. C. Ahalt, "Classification of radar targets using synthetic neural networks," *IEEE Trans. Aerosp. Electron. Syst.*, vol. 29, no. 2, pp. 336-344, Apr. 1993.
- [12] E. C. Botha, E. Barnard, and C. J. Barnard, "Feature-based classification of aerospace radar targets using neural networks," *Neural Netw.*, vol. 9, no. 1, pp. 129-142, Jan. 1996.
- [13] G. Sun, J. Wang, S. Qin, and J. Na, "Radar target recognition based on the multi-resolution analysis theory and neural network," *Pattern Recogn. Lett.*, vol. 29, no. 16, pp. 2109-2115, Dec. 2008.
- [14] J. S. Kobashigawa, H.-S. Youn, M. F. Iskander, and Z. Q. Yun, "Classification of buried targets using ground penetrating radar: Comparison between genetic programming and neural networks," *IEEE Antennas Wirel. Propag. Lett.*, vol. 10, pp. 971-974, 2011.
- [15] F. A. Sadjadi, "Polarimetric radar target classification using support vector machines," *Opt. Eng.*, vol. 47, no. 4, 046201, Apr. 2008.
- [16] Q. Zhao and J. C. Principe, "Support vector machines for SAR automatic target recognition," *IEEE Trans. Aerosp. Electron. Syst.*, vol. 37, no. 2, pp. 643-654, Apr. 2001.
- [17] M. A. Selver, M. M. Taygur, M. Secmen, and E. Y. Zoral, "Hierarchical reconstruction and structural waveform analysis for target classification," *IEEE Trans. Antennas and Propagation*, vol. 64, no. 7, pp. 3120-3129, July 2016.
- [18] M. A. Selver, M. Secmen, and E. Y. Zoral, "Comparison of scattered signal waveform recovery techniques under low SNR for target identification," *European Conference on Antennas and Propagation (EUCAP) 2017*, pp. 1091-1095, Paris, France, Mar. 2017.
- [19] S. J. Wang and J. L. Lai, "Geometrical learning, descriptive geometry, and biomimetic pattern recognition," *Neurocomputing*, vol. 67, pp. 9-28, Aug. 2005.
- [20] S. J. Wang, "Computational information geometry and its applications," in *Conf. Rec. 2005 IEEE Int. Conf. Neural Networks and Brain*, pp. PL-63-9, Oct. 2005.
- [21] L. Wang, L. D. Xu, R. J. Liu, and H. H. Wang, "An approach for moving object recognition based on BPR and CI," *Inf. Syst. Front.*, vol. 12, no. 2, pp. 141-148, Apr. 2010.
- [22] M. Secmen and G. Turhan-Sayan, "An electromagnetic target classification method for the target sets with alien target: Application to small-scale aircraft targets," *PIERS Online*, vol. 6, no. 5, pp. 425-429, 2010.
- [23] M. Secmen, "Novel Music Algorithm based Electromagnetic Target Recognition Method in Resonance Region for the Classification of Single and Multiple Targets," *Ph.D. dissertation*, Dept. Elect. Electron. Eng., Middle East Tech. Univ., Ankara, Turkey, 2008.
- [24] R. G. Kouyoumjian, "Asymptotic high-frequency methods," *Proc. IEEE*, vol. 53, no. 8, pp. 864-876, Aug. 1965.
- [25] A. B. Gorji, B. Zakeri, and R. C. Janalizadeh, "Physical optics analysis for RCS computation of a relatively small complex structure," *Applied Computational Electromagnetics Society Journal*, vol. 29, no. 7, pp. 530-540, Dec. 2014.
- [26] F. Weinmann, "UTD shooting-and-bouncing extension to a PO/PTD ray tracing algorithm," *Applied Computational Electromagnetics Society Journal*, vol. 24, no. 3, pp. 281-293, June 2009.
- [27] C. Cortes and V. Vapnik, "Support-vector network," *Mach. Learn.*, vol. 20, no. 3, pp. 273-297, Sept. 1995.
- [28] C. C. Chang and C. J. Lin, "LIBSVM: A library for support vector machines," *ACM Trans. Intell. Syst. Technol.*, vol. 2, no. 3, Article 27, Apr. 2011. Software Available: <http://www.csie.ntu.edu.tw/~cjlin/libsvm>
- [29] C. W. Hsu, C. C. Chang, and C. J. Lin, "A practical guide to support vector classification," Apr. 2010. Available : <http://www.csie.ntu.edu.tw/~cjlin/libsvm>



**Huan Huan Zhang** received the Ph.D. degree in Electromagnetic Fields and Microwave Technology from Nanjing University of Science and Technology in 2015. He was a Postdoctoral Research Fellow with the Center of Electromagnetics and Optics, the University of Hong Kong, Hong Kong, from 2015 to 2016. He is currently a

Lecturer with the School of Electronic Engineering, Xidian University, Xi'an, China.

Zhang serves as the Reviewer of the IEEE Transactions on Antenna and Propagation, Communications in Computational Physics, IEEE Microwave and Wireless Components Letters, IEEE ACCESS, IET Radar, Sonar & Navigation, Applied Computational Electromagnetic Society Journal, etc. His current research interests include multiphysics simulation, computational electromagnetics, and radar signal processing.



signal processing.

**Pei Yu Chen** received the bachelor's degree from Luoyang Normal University in 2016. Now she is working towards the master's degree in Electromagnetic Fields and Microwave Technology at Xidian University. Her current research interests include multiphysics simulation and radar